

# Ultrasonic Characterization of Water Sorption in Poly(2-hydroxyethyl methacrylate) Hydrogels

A. MAFFEZZOLI,<sup>1</sup> A. M. LUPRANO,<sup>2</sup> G. MONTAGNA,<sup>2</sup> L. NICOLAIS<sup>3</sup>

<sup>1</sup> Department of Materials Science, University of Lecce Via per Arnesano, 73100 Lecce, Italy

<sup>2</sup> PASTIS-CNRSM, SS 7, Km 714, 72100, Brindisi, Italy

<sup>3</sup> Department of Materials and Production Engineering University of Naples Federico II, P. Tecchio 80125 Naples, Italy

Received 9 January 1997; accepted 8 August 1997

**ABSTRACT:** A complex mechanism characterizes the water uptake kinetics in hydrogels, as a consequence of the strong structural changes occurring in the material during the sorption process. The water sorption involves the transformation of a glassy, moderately crosslinked polymer in a rubbery material. In this study, the changes in the ultrasonic attenuation and velocity in crosslinked poly(2-hydroxyethyl methacrylate) [poly-(HEMA)] hydrogel films during water sorption are measured by scanning laser acoustic microscopy (SLAM) and a pulse–echo system. In particular, the pulse–echo technique provides additional valuable information, thanks to its capability for monitoring the position of the swollen/unswollen fronts during water sorption. The evolution of the attenuation observed by SLAM is analyzed in terms of reflections on macroscopic discontinuities and absorption mechanisms. Finally, the propagation of ultrasonic waves acts as a dynamic mechanical test of the material; and, therefore, the measured longitudinal velocity and ultrasonic attenuation are applied to the calculation of the storage bulk longitudinal modulus of the poly(HEMA) hydrogels during water sorption. © 1998 John Wiley & Sons, Inc. *J Appl Polym Sci* **67**: 823–831, 1998

**Key words:** hydrogels; sorption kinetics; ultrasonic velocity; ultrasonic attenuation

## INTRODUCTION

The kinetics of water sorption in dry hydrogel films is characterized by the swelling of the glassy matrix in correspondence of two fronts moving from the sample boundaries towards the center and separating a glassy core from two external rubbery regions. Water acts as a plasticizer, reducing the glass transition temperature ( $T_g$ ) of the polymer below the sorption temperature and determining a glass transition in the polymer.<sup>1–3</sup> The discontinuity in the material properties at the glassy–rubbery fronts is responsible for the reflections of the elastic waves propagating

through the hydrogel. Furthermore, ultrasonic waves act as a high-frequency dynamic–mechanical deformation applied to the material; and the acoustic attenuation and velocity may be used for the calculation of both the loss and storage bulk moduli and the loss factor of the hydrogel during water sorption.<sup>4–6</sup> In particular, the acoustic attenuation is a measure of the energy loss as the wave travels through the polymer and is directly correlated with the loss factor.

The evolution of the attenuation during water sorption in poly(hydroxyethyl methacrylate) [poly(HEMA)] hydrogels measured by scanning laser acoustic microscopy (SLAM) is presented in previous papers.<sup>7,8</sup> The behavior was qualitatively analyzed in terms of reflections at the external boundaries of the sample and at the two swollen/unswollen interfaces moving across the sample,

---

Correspondence to: A. Maffezzoli.

and in terms of absorption mechanism. The qualitative comparison of the reflection function with the experimental data indicated that the absorption mechanism dominates the time dependence of attenuation. It must be considered that the kinetics of water sorption in dry hydrogels determines a glass transition in the polymer at the swollen/unswollen fronts and that a strong energy absorption occurs in correspondence of a  $T_g$  in a polymer subject to a dynamic deformation. The energy absorption at  $T_g$  is observed in dynamic mechanical experiments as a peak in the loss factor or in the damping factor; in dielectric experiments as a peak in the dielectric loss; and, finally, in acoustic wave propagation as a peak in the acoustic attenuation. In the former works<sup>7,8</sup> the time dependence of acoustic velocity, measured by a pulse–echo system, was also presented. The velocity showed a continuous decrease as the mechanical properties and the density of the hydrogel changed from that of a glass to that of a rubber during water sorption.

In this work, the potential of pulse–echo measurements for monitoring the swollen/unswollen front position during water sorption in poly-(HEMA) hydrogels is reported. The relative changes in the ultrasonic attenuation and velocity measured by SLAM and the pulse–echo technique, respectively, are applied to the quantitative determination of the contributions of reflection and absorption mechanisms to the measured attenuation. Finally, the potential of ultrasonic measurements as an *in situ* and nondestructive dynamic mechanical analysis technique is analyzed.

## EXPERIMENTAL

The poly(HEMA) hydrogel films are prepared as already reported in a former article.<sup>7</sup> Each sample of constant thickness was cut in three parts used for each of the three types of measurements performed.

After drying, the samples under vacuum at 90°C for 12 h, ultrasonic and thickness measurements during water sorption are performed by immersion of the samples in distilled water (used also as a coupling fluid for ultrasonic waves transmission) at a constant temperature of 25°C. Since the samples are characterized by a thin film geometry (with an aspect ratio larger than 20 : 1), a one-dimensional water sorption process is assumed.

## SLAM Measurements

Ultrasonic wave attenuation is measured by a SLAM 2160 system manufactured by Sonoscan, Chicago, IL. The SLAM system uses a piezoelectric transducer to produce plane continuous ultrasonic waves at the frequencies of 10 and 30 MHz and a scanning laser beam to detect the amplitude of the ultrasonic waves after their propagation inside the sample. Absorption, scattering, or reflection of the ultrasonic waves crossing the sample are due to changes of the elastic properties and of the density of the sample. Acoustic attenuation measurements are made by means of a comparison technique. Having the sample in place and the acoustic image displayed on the CRT, the appropriate region of interest is selected. The relative image brightness in this region, compared to that when no material is present, is a measure of the attenuation.

## Pulse–Echo Measurements

The longitudinal velocity and the ultrasonic wave attenuation during the water absorption are also measured by pulse–echo measurements at the frequencies of 20 MHz by using a Panametrics 560A1-ST system connected with an oscilloscope Philips PM3323.

It must be highlighted that the SLAM system operates in a transmission mode: a transducer produces the ultrasonic waves on one side of the sample, and a laser system detects the waves on the other side. On the other hand, in the pulse–echo system, the piezoelectric transducer, producing a pulsed plane ultrasonic wave, operates also as a receiver (reflection mode) of the echoes occurring in correspondence of any eventual macroscopic discontinuity across the sample.

## TMA Measurements

Thickness measurements are performed on a sample of the same thickness of the ones used in the ultrasonic characterization by means of Thermomechanical analyzer (TMA) 402 manufactured by Netzsch (Selb, Germany). In order to avoid the penetration of the TMA probe into the rubbery film, a net characterized by a large mesh is placed between the sample and the probe. The measurements are carried out keeping the poly-(HEMA) film into the water at the same temperature used for the ultrasonic characterization.

## RESULTS AND DISCUSSION

### Fronts Position and Velocity Measurements

The analysis of water sorption by the pulse–echo system provides further valuable information with respect to the ones presented in the former articles.<sup>7,8</sup> The hard copy of the oscilloscope, reporting the amplitude of the reflected wave as a function of the flight time (that represents the time that the wave pulse needs to reach a discontinuity and to return back to the transducer) is shown in Figure 1(a–c) at different sorption times. Figure 1(a) clearly shows that reflections occur during water sorption at the two moving swollen/unswollen interfaces. In Figure 1(a), four echoes are clearly shown. The first one occurs at the boundary of the sample when the ultrasonic pulse goes from the water into the sample. The two fronts between the rubbery boundaries and the glassy core, during water sorption in poly(HEMA), are responsible for the second and third reflections of the ultrasonic waves. Finally, the fourth echo occurs at the sample boundary on the opposite side of the transducer. A sketch of water sorption process in poly(HEMA) hydrogels and the multiple reflections occurring during propagation of ultrasonic wave are reported in Figure 2.

The attenuation is qualitatively observed as a reduction of the absolute value of the reflection peaks as the ultrasonic pulse goes through the different discontinuities across the material. From Figure 1(a) is also evident the change of phase of the acoustic signal occurring when the wave travels from the glassy core to the second rubbery portion of the sample. This phase change is the consequence of the transmission of the wave from a material characterized by a high acoustic impedance, the glassy hydrogel core, to a material characterized by a low acoustic impedance, the rubbery swollen external part of the sample film.<sup>9</sup> The acoustic impedance of a material  $Z$  is given by the product of the density  $\rho$  and of the characteristic sound velocity  $v$ , as follows:

$$Z = \rho v \quad (1)$$

As the two swollen/unswollen fronts move towards the center of the sample, the second and third reflections overlap [Fig. 1(b)] and cannot be distinguished anymore. This occurs when the thickness of the dry glassy core of the sample reduces to a value comparable to that of ultrasonic wavelength. In Figure 1(c), corresponding to a sorption time close to the sample saturation, the

dry core disappears; and only two reflections at the two sample boundaries are detected. Comparing parts (a)–(c) of Figure 1, it is evident that the flight times corresponding to the fourth reflection becomes higher as the sorption time increases. The longitudinal velocity, calculated taking into account even the increase of the thickness measured by TMA (Fig. 3), decreases as the rubbery phase in the film becomes thicker.

The ultrasonic velocity can be calculated with respect of each of the reflections occurring at the discontinuities in the sample. An average velocity  $v_a$  is obtained combining the flight time  $\tau_f$  of the fourth reflection [Fig. 1(a)], corresponding to a wave that travels throughout the sample, with the thickness changes measured by TMA (Fig. 3), as follows:

$$v_a = 2h(t)/\tau_f \quad (2)$$

where  $h(t)$  is the time-dependent sample thickness.  $v_a$  as a function of the sorption time, reported in Figure 4, shows a continuous decrease up to the saturation as the elastic properties of the glassy polymer move towards the ones of a soft rubbery material. A lack of data close to the time instant in which the glassy core disappears is due to interference phenomena between the echoes.

The ultrasonic velocity in the swollen rubbery polymer before the glassy core disappears could also be calculated by using the second echo of Figure 1(a,b). However, it is necessary to establish the time dependence of the thickness of the first rubbery layer.

Two positions ( $x$  direction) are definitely known for the swollen/unswollen front closer to the transducer, as follows:

$$\text{for } t = 0 \quad x = 0 \quad (3)$$

$$\text{for } t = t_r \quad x = h/2 \quad (4)$$

where  $t_r$  is the time corresponding to the disappearance of the glassy core and, hence, of the two central peaks; and  $x$  the coordinate along the thickness. Two limiting behaviors, as follows, may be assumed between these two points:

$$x = kt \quad (5)$$

$$x = kt^{0.5} \quad (6)$$

Equation (5) corresponds to the case II sorption process, while eq. (6) to a Fickian behavior.<sup>1,10,11</sup>

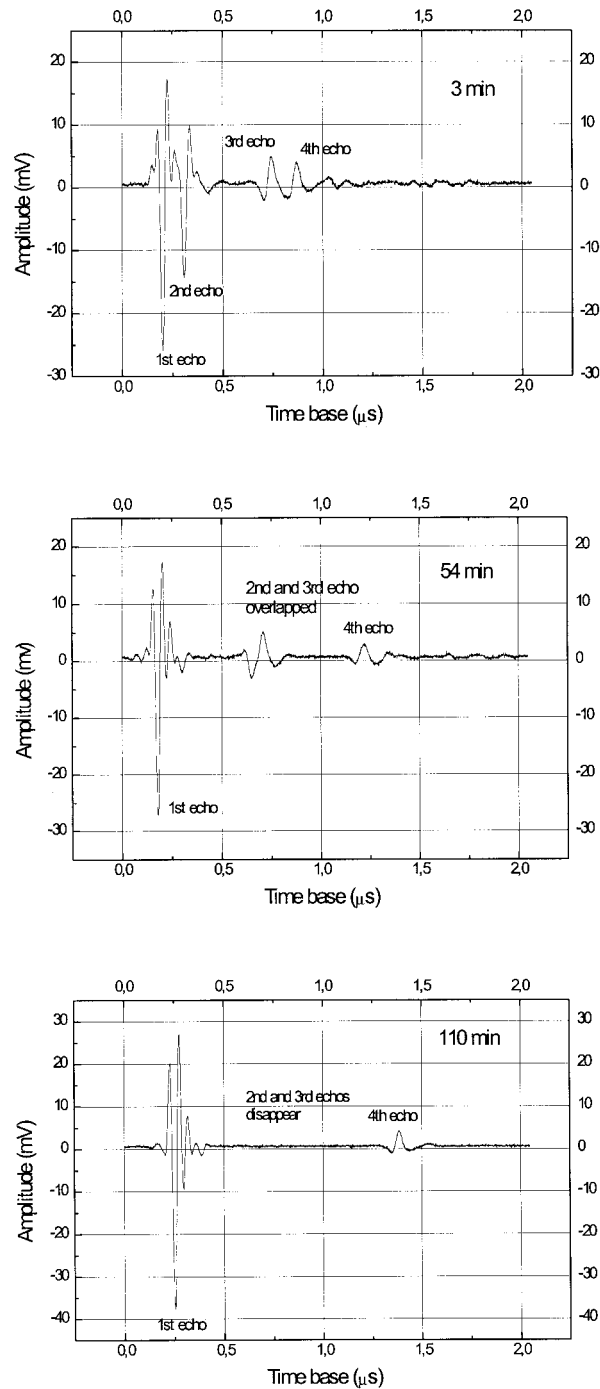


**Figure 1** Acoustic signal visualized on the oscilloscope at three different times during the advancements of the fronts in a 0.86-mm-thick sample.

The velocity obtained applying eqs. (5) and (6) are reported in Figure 5. Taking into account that the acoustic velocity in water is about 1490 m/s, it is evident that the values obtained using eq. (5) have no physical meaning. On the other hand, a constant value of the ultrasonic velocity of about

1700 m/s is obtained applying eq. (6). These results suggest that the advancement of the swollen/unswollen fronts follows a square root dependence on the sorption time and, hence, an apparent Fickian behavior. Although the strong polymer–water specific interaction occurring in

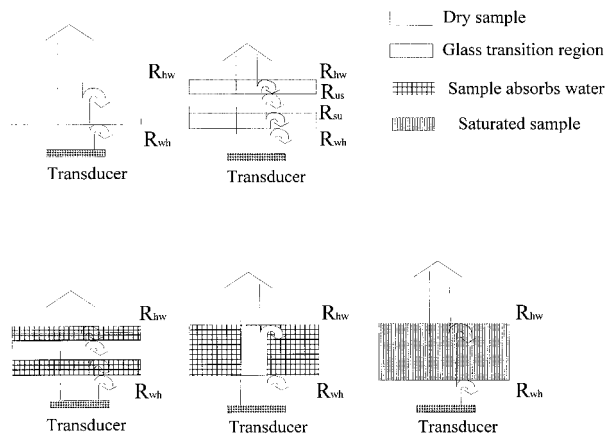


**Figure 2** Sketch of a poly(HEMA) film indicating the different stages of the water sorption process.

hydrogels should generally lead to a case II sorption behavior,<sup>10,11</sup> the normalized weight gain data show a linear dependence on  $t^{0.5}$ . This behavior is usually explained assuming that the water dissolution in the swollen rubbery matrix, governed by a Fickian behavior, is the rate-limiting step.<sup>1-3,12,13</sup>

It should be noted that the ultrasonic velocity and, hence the elastic properties of the polymer, abruptly decreases from the value of 3000 m/s of the glass to about 1800 m/s of the rubber across the swollen/unswollen front. Furthermore, the calculated velocity of Figure 5 for the rubbery portion of the water-absorbing hydrogel is very close to the value of  $v_a$  (Fig. 4) calculated when the material is saturated. Then,  $v_a$  represents an average value for a multilayer system and is essentially affected by the thickness of the glassy core.

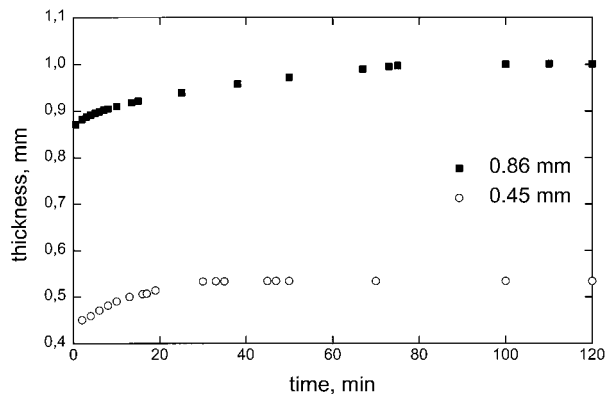


**Figure 3** Hydrogel swelling measured by TMA during water sorption for samples 0.45 and 0.86 mm thick.

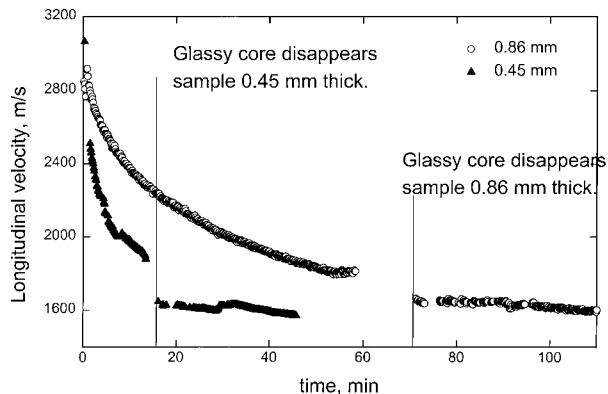


**Figure 4** Ultrasonic longitudinal velocity for the 0.45- and 0.86-mm-thick samples as a function of the sorption time.

**Attenuation Measurements**

The insertion losses  $\alpha'$  through a given sample are measured by SLAM experiments as the ratio between the amplitude of the acoustic wave going into the sample  $A_o$  and the amplitude  $A_T$  transmitted on the opposite side of the sample. Usually  $\alpha'$  is measured in decibel (dB) as follows<sup>9</sup>:

$$\alpha' = 10 \text{ Log}[(A_o/A_T)] \tag{7}$$

SLAM experiments were applied to the determination of the insertion losses of poly(HEMA) samples, with different thicknesses, during water sorption, as shown in Figure (6). The measurements performed on the 0.45 mm thick sample are characterized by an attenuation peak, while a plateau is observed in Figure (6) for the thicker sample. In both cases, after an initial increase,

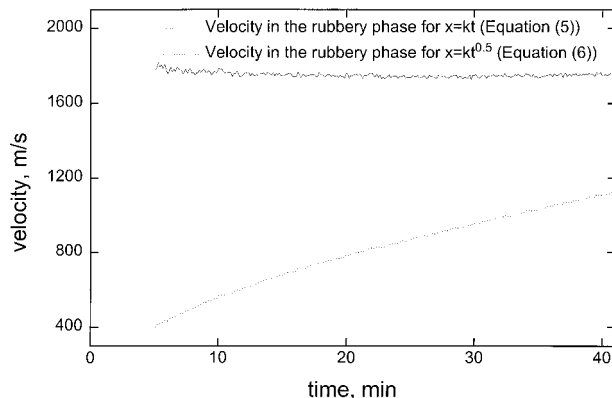


**Figure 5** Ultrasonic velocity calculated in the swollen portion of the hydrogel using eqs. (5) and (6).

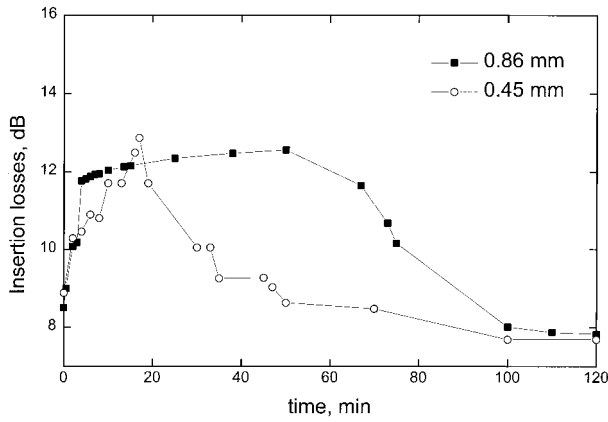


**Figure 6** Total ultrasonic attenuation for the 0.45- and 0.86-mm-thick samples as a function of the sorption time.

the ultrasonic attenuation drops to its lowest value when the hydrogel is saturated. It should be noted that, as mentioned in the experimental section, SLAM data must be considered in terms of relative changes.

The dependence of the insertion losses  $\alpha'$  from the water sorption was interpreted in terms of reflection, scattering, and absorption mechanisms in previous works.<sup>7,8</sup> However, the scattering contribution was already analyzed and considered negligible. On the other hand, further considerations have to be done on the reflection and absorption contributions. In SLAM experiments, the ratio between the amplitude  $A_T$  of the acoustic wave transmitted through the sample and the amplitude of the wave entering into the sample on the opposite side  $A_o$  is given by a combination of reflections and absorption effects. When the hydrogel is dry or fully rubbery, the reflections may occur only at the hydrogel boundaries; and the ratio  $A_T/A_o$  is given by

$$A_T/A_o = (1 - R_{wh})(1 - R_{hw})\exp[-\alpha_h h(t)] \quad (8)$$

where  $R_{wh}$  and  $R_{hw}$  are the reflection coefficients at the water–hydrogel and hydrogel–water boundaries, respectively, calculated from their acoustic impedances<sup>6,8</sup>;  $\alpha_h$  is the absorption component of the attenuation coefficient; and  $h(t)$  is the sample thickness, dependent on the sorption time (Fig. 1). At the beginning of the water sorption process, the two additional interfaces between the swollen and unswollen hydrogel must be considered; and eq. (8) is modified as follows:

$$A_T/A_o = (1 - R_{hw})(1 - R_{su})(1 - R_{us}) \\ \times (1 - R_{wh})\exp[-\alpha_h h(t)] \quad (9)$$

where  $R_{su}$  and  $R_{us}$  are the reflection coefficients at the swollen–unswollen and unswollen–swollen interfaces, respectively. The absorption component of the attenuation coefficient  $\alpha_h$  may be calculated from eqs. (8) and (9) once the  $R_{ij}$  are calculated as a function of the acoustic impedance. The functions  $R_{ij}$  in eqs. (8) and (9) are calculated assuming that the ultrasonic velocity is 3000 m/s in the dry material, 1800 m/s (Fig. 4) in the rubbery material during the front advancement; and 1600 m/s in the saturated hydrogel. The attenuation is obtained from eqs. (8) or (9) during water sorption, depending on the number of interfaces encountered on the transmission path by the acoustic waves. In particular,  $\alpha_h$  is calculated using eq. (8) at time  $t = 0$  for the dry hydrogel, then using eq. (9) until the attenuation reaches the maximum (17 min for the data of Fig. 6). For the last part of the experiment,  $\alpha_h$  is calculated using again eq. (8), applied to the swollen hydrogel. In other words, the attenuation is calculated first using eq. (8); then eq. (9); and, finally again, eq. (8), assuming that the two central discontinuities suddenly disappear in correspondence of the maximum of  $\alpha'$  in Figure 6. However, this is a quite rough approximation of the real process since, as shown in Figure 1, the two central echoes first overlap and then disappear in a finite time interval; and, hence, the corresponding reflections decrease slowly as the glassy core reaches a thickness of the same order of the wavelength.

The transmitted fraction of the acoustic waves depends on two distinct contributions: reflections at each interface, and material absorption. In order to compare these contributions using homogeneous quantities, the transmitted fraction arising from the contribution of the reflections,  $(A_T/A_o)_{Ti}$ , is calculated for a single or triple layer sample, respectively, as follows:

$$(A_T/A_o)_{T1} = (1 - R_{hw})(1 - R_{wh}) \quad (10)$$

$$(A_T/A_o)_{T2} = (1 - R_{hw})(1 - R_{su}) \\ \times (1 - R_{us})(1 - R_{wh}) \quad (11)$$

Once  $\alpha_h$  is calculated from eqs. (8) and (9), as described above, the transmitted fraction arising from the contribution of absorption  $(A_T/A_o)_\alpha$  is given by

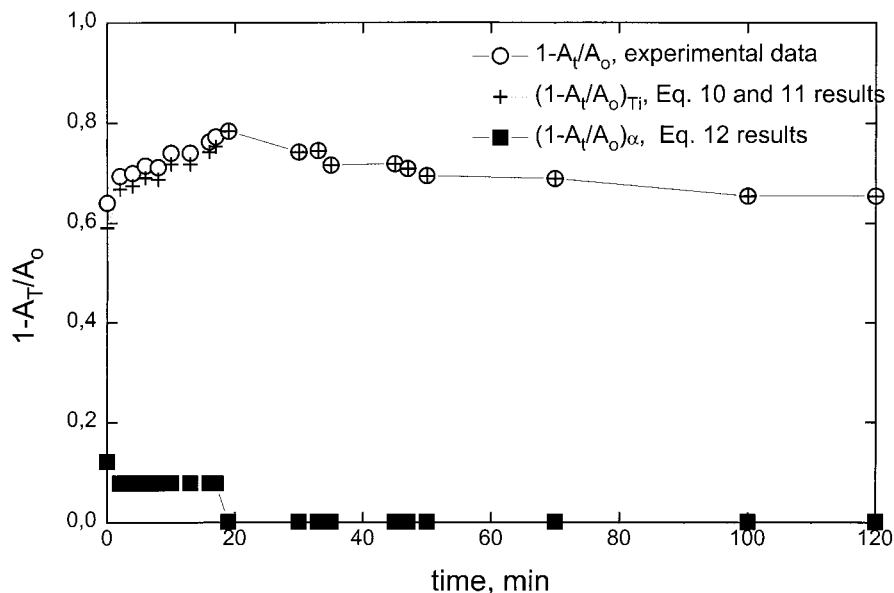


**Figure 7** Comparison of the relative contributions of reflections and absorption to the total losses for a 0.45-mm-thick sample as a function of the sorption time.

$$(A_T/A_o)_\alpha = \exp[-\alpha_h h(t)] \quad (12)$$

Now the correspondent reflected and absorbed fraction for each mechanism, represented by  $1 - (A_T/A_o)_{T1}$  or  $1 - (A_T/A_o)_{T2}$ , and by  $1 - (A_T/A_o)_\alpha$ , respectively, are compared with the total losses,  $1 - A_T/A_o$ , given by eqs. (8) or (9), in Figure 7, for the 0.45 mm thick sample. As shown in this figure, the two terms  $1 - A_T/A_o$  and  $1 - (A_T/A_o)_\alpha$ , presenting the same time dependence of  $\alpha'$  in Figure 6, are very close and assume almost equal values when the glassy core disappears; and the reflections drop to very small values. The very limited reflections occurring in the last part of the sorption process depend on the very close values of the acoustic impedances of the water and of the swollen hydrogel. The comparison of the relative values of  $1 - A_T/A_o$ ,  $1 - (A_T/A_o)_{Ti}$ , and  $1 - (A_T/A_o)_\alpha$  indicates that the evolution of the total attenuation reported in Figure 6 must be essentially attributed to an energy absorption mechanism, occurring as a consequence of the glass transition induced by the plasticizing action of the water, rather than to the reflections at the additional swollen–unswollen interfaces. The difference between the initial and maximum values of insertion losses in Figure 6 is the same for both thicknesses. This further indicates that the relative change in the attenuation must be attributed to a solvent-activated glass transition independently from the sample thickness.

Therefore, the effect of water sorption on the attenuation coefficient is related to the development of two regions, where a glass–rubber transition occurs. When the two swollen rubbery layers are formed, more water is absorbed in the rubbery phase, according to a Fickian mechanism.<sup>1–3,11–13</sup> For the thicker sample, the attenuation, after the initial increase, levels to a constant value, corresponding to the development of two moving regions of constant thickness, undergoing a glass transition and crossing the sample from the boundaries toward the center, as shown in Figure 6. In this last case, the thickness of the regions undergoing the glass transition is lower than the half-thickness of the sample (i.e., 0.43 mm). When the glassy core disappears, as detected by the pulse–echo method, the glass–rubber transition is completed throughout the thickness; and water is absorbed only in the swollen rubbery matrix. Finally, the ultrasonic attenuation decreases to a final value lower than the initial one as the acoustic impedances of the water and of the swollen hydrogel become very close.

### Dynamic Mechanical Behavior

The measurements of ultrasonic velocity and attenuation may be used for the calculation of the storage ( $M'$ ) and loss ( $M''$ ) bulk longitudinal moduli.<sup>4–6</sup>  $M'$  and  $M''$  may be calculated according to the following equations<sup>6</sup>:

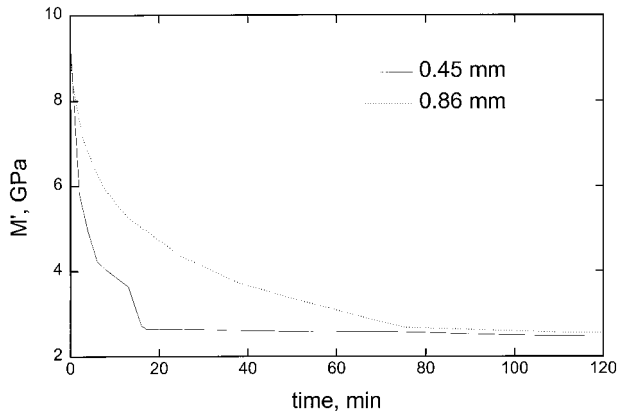


**Figure 8** Storage modulus for the 0.45- and 0.86-mm-thick samples as a function of the sorption time.

$$M' = \frac{\rho v_a^2 \left[ 1 - \left( \frac{\alpha_h \lambda}{2\pi} \right)^2 \right]}{\left[ 1 + \left( \frac{\alpha_h \lambda}{2\pi} \right)^2 \right]^2} \quad (12)$$

$$M'' = \frac{2\rho v_a^2 \left( \frac{\alpha_h \lambda}{2\pi} \right)}{\left[ 1 + \left( \frac{\alpha_h \lambda}{2\pi} \right)^2 \right]^2} \quad (13)$$

where  $\rho$  is the material density;  $\lambda$  is the wavelength, given by  $\lambda = v_a/f$  as a function of the frequency  $f$ ; and  $\alpha_h$  is calculated from eqs. (8) and (9), as indicated in the former paragraph. These moduli are related to the bulk ( $K'$  and  $K''$ ) and shear ( $G'$  and  $G''$ ) moduli,<sup>6</sup> as follows:

$$M' = K' + \frac{4}{3}G' \quad (14)$$

$$M'' = K'' + \frac{4}{3}G'' \quad (15)$$

$M'$  corresponds to the stiffness of a deformed system, changing its dimensions in one direction; while, in the other two directions, the dimensions are constrained to be constant. For a soft rubbery material,  $K' \gg G'$ , and  $M'$  may be considered equal to the bulk modulus,<sup>6</sup> but  $K''$  and  $G''$  may be of the same order of magnitude, and the effect of  $G''$  may not be neglected. The changes of  $M'$  and  $M''$  as a function of the temperature or of the frequency are not easily interpreted<sup>6</sup> as a consequence of their complex nature, arising from the combination of bulk and shear moduli.  $M'$  is calculated from eq. (12) and reported in Figure 8 for

the two different sample thicknesses as a function of the sorption time. The fast decrease of  $M'$  in Figure 8 may be essentially attributed to the dramatic decrease of  $G'$  occurring when a rubbery soft phase appears at the beginning of the water sorption process [eq. (14)]. The decrease of  $K'$  across the glass transition is usually quite small<sup>6</sup>; while  $M'$  reduces of about five times, indicating that the change in  $G'$  dominates the evolution of  $M'$ . Therefore, the final values of  $M'$  may be considered as a measure of the bulk modulus of the hydrogels.

## CONCLUSIONS

In this study, the evolution of the acoustic attenuation and velocity during water sorption of a poly-(HEMA) hydrogel has been monitored. In particular, the pulse-echo technique is applied to the monitoring of the swollen-unswollen fronts position during water sorption. The calculation of ultrasonic velocity in the swollen portion of the hydrogel leads to the conclusion that the advancement of the swollen-unswollen fronts follows a square root dependence on the sorption time according to an apparent Fickian behavior. The evolution of the attenuation observed by SLAM is analyzed in terms of reflections on macroscopic discontinuities and absorption mechanisms. The quantitative comparison of the contributions of absorption and reflections indicated that the absorption mechanisms are largely responsible for the time dependence of the total attenuation. Moreover, the propagation of ultrasonic waves acts as a dynamic mechanical test of the material; therefore, the measured longitudinal velocity and ultrasonic attenuation may be applied to the calculation of the storage and loss bulk longitudinal moduli of an hydrogel during water sorption. In particular, the modulus  $M'$  for soft materials like swollen hydrogels is a measure of their bulk modulus.

The measurements of the evolution of acoustic attenuation during water sorption in a hydrogel show a strong potential in the field of controlled release of drugs. In devices activated and controlled by solvents, the environmental fluid penetrates the matrix that swells the polymer and allows the drug contained in it to diffuse through the polymer. The rate of release depends on the swelling kinetics and therefore on the rate of advancement of the glass-rubber front through the hydrogel. This technique, representing a nondestructive tool for the detection of the moving



fronts, may be applied to the study of the solvent activated–controlled devices for drug release.

The authors thank the Panametrics Co., which supplied the pulse–echo probe, and Dr. R. Terzi and M. Schioppa for the thickness measurements.

## NOMENCLATURE

$Z$	acoustic impedance
$\rho$	material density
$v$	ultrasonic longitudinal velocity
$v_a$	average ultrasonic longitudinal velocity through rubbery and glassy regions
$h$	sample thickness
$\tau_f$	flight time
$t$	sorption time
$x$	coordinate along the thickness
$t_r$	time corresponding to disappearance of the glassy core
$\alpha'$	insertion losses
$A_o$	amplitude of the acoustic wave going into the sample
$A_T$	amplitude transmitted through the sample
$R_{wh}$	reflection coefficient at the water–hydrogel boundary
$R_{hw}$	reflection coefficient at the hydrogel–water boundary
$R_{su}$	reflection coefficient at the swollen–unswollen boundary
$R_{us}$	reflection coefficient at the unswollen–swollen boundary
$\alpha_h$	absorption component of the attenuation coefficient
$f$	ultrasonic frequency
$G'$	storage shear modulus

$G''$	loss shear modulus
$K'$	storage bulk modulus
$K''$	loss bulk modulus
$M'$	storage bulk longitudinal modulus
$M''$	loss bulk longitudinal modulus
$\lambda$	ultrasonic wavelength

## REFERENCES

1. N. A. Peppas and R. W. Kormsmeier, in *Hydrogels in Medicine and Pharmacy*, Vol. III, N. A. Peppas, Ed., CRC Press, Boca Raton, 1987, Chap. 6.
2. P. W. R. Davidson and N. A. Peppas, *J. Controlled Release*, **3**, 243 (1986).
3. C. Migliaresi, L. Nicodemo, L. Nicolais, and P. Passerini, *J. Biomed. Mater. Res.*, **15**, 307 (1981).
4. I. Perepechko, *Acoustic Methods of Investigating Polymers*, Mir Publishers, Moscow, 1975.
5. D. W. Van Krevelen, *Properties of Polymers*, Elsevier, Amsterdam, 1990.
6. J. D. Ferry, *Viscoelastic Properties of Polymers*, Wiley, New York, 1980.
7. A. Maffezzoli, V. Luprano, F. Esposito G. Montagna, and L. Nicolais, *Polym. Eng. Sci.*, **36**, 1832 (1996).
8. V. A. M. Luprano, A. Maffezzoli, and G. Montagna, *IEEE Ultras., Ferroelec., Freq. Control Soc. Trans.*, **43**, 948 (1996).
9. J. Krautkramer and H. Krautkramer, *Ultrasonic Testing of Materials*, Springer-Verlag, Berlin, 1977.
10. M. A. Del Nobile, G. Mensitieri, P. A. Netti, L. Nicolais, *Chem. Eng. Sci.*, **49**, 633 (1994).
11. A. H. Windle, in *Polymer Permeability*, J. Comyn, Ed., Elsevier, London, 1985.
12. C. Migliaresi, L. Nicodemo, L. Nicolais, and P. Passerini, *Polymer*, **25**, 686 (1984).
13. L. B. Peppas and N. A. Peppas, *Biomaterials*, **11**, 635 (1990).
14. J. Tatibouet and L. Pichè, *Polymer*, **32**, 3147 (1991).